Intrinsic peroxidase-like activity of ferromagnetic nanoparticles

LIZENG GAO[1,2,3†], JIE ZHUANG[1,2,3†], LENG NIE[3,4], JINBIN ZHANG[1,2,3], YU ZHANG[5], NING GU[5], TAIHONG WANG[4], JING FENG[1,2], DONGLING YANG[1,2], SARAH PERRETT[1*] AND XIYUN YAN[1,2*]

[1]National Laboratory of Biomacromolecules, Institute of Biophysics, Chinese Academy of Sciences, 15 Datun Road, Beijing 100101, China
[2]Chinese Academy of Sciences–University of Tokyo Joint Laboratory of Structural Virology and Immunology, Institute of Biophysics, Chinese Academy of Sciences, 15 Datun Road, Beijing 100101, China
[3]Graduate School of the Chinese Academy of Sciences, Beijing 100049, China
[4]Institute of Physics, Chinese Academy of Sciences, Beijing 10080, China
[5]State Key Laboratory of Bioelectronics, Southeast University, Nanjing 210096, China
[†]These authors contributed equally to this work
*e-mail: sarah.perrett@iname.com; yanxy@sun5.ibp.ac.cn

Published online: 26 August 2007; doi:10.1038/nnano.2007.260

Nanoparticles containing magnetic materials, such as magnetite (Fe_3O_4), are particularly useful for imaging and separation techniques. As these nanoparticles are generally considered to be biologically and chemically inert, they are typically coated with metal catalysts, antibodies or enzymes to increase their functionality as separation agents. Here, we report that magnetite nanoparticles in fact possess an intrinsic enzyme mimetic activity similar to that found in natural peroxidases, which are widely used to oxidize organic substrates in the treatment of wastewater or as detection tools. Based on this finding, we have developed a novel immunoassay in which antibody-modified magnetite nanoparticles provide three functions: capture, separation and detection. The stability, ease of production and versatility of these nanoparticles makes them a powerful tool for a wide range of potential applications in medicine, biotechnology and environmental chemistry.

There is currently intense interest in the use of nanoparticles for a wide range of biomedical and technological applications. Among known nanomaterials, magnetic nanoparticles (MNPs) are of particular interest because of their power in biological imaging or separation techniques. For instance, MNPs have been used for separating proteins, DNA and cells from samples[1,2], for drug and gene targeting[3], for tissue engineering[4], for magnetic resonance imaging[5–7], as magnetic biosensors[8], and as mediators of heat for cancer therapy (hyperthermia)[9]. Nanoparticles are generally considered to be biologically and chemically inert. Magnetic nanoparticles (such as Fe_3O_4) have been coated with metal catalysts or conjugated with enzymes, to combine the separating power of the magnetic properties with the catalytic activity of the metal surface or enzyme conjugate[10–13]. For example, horseradish peroxidase (HRP)-entrapped magnetic nanoparticles have been used for biocatalysis and bioseparation[14], and a magnetic core of Co coated with Pt allows magnetic separation and catalysis of hydrogenation[15]. These dual-functional nanoparticles are composed of two parts: their cores provide a magnetic function and their shells allow catalysis.

In this study, we made the surprising discovery that Fe_3O_4 nanoparticles possess intrinsic peroxidase-like activity. Peroxidase activity has a wide range of practical applications. For example, the ability to catalyse the oxidation of organic substrates to reduce their toxicity and/or to produce a colour change is frequently used in wastewater treatment or as a detection tool. From a chemical point of view, our finding is not unexpected, as Fe^{2+}/Fe^{3+} ions in solution (Fenton's reagent) are known to catalyse the breakdown of hydrogen peroxide. Furthermore, a number of peroxidase enzymes (including the haem-containing enzyme HRP) and enzyme mimetics also contain Fe^{2+} or Fe^{3+} in their reaction centres[16–19]. However, the fact that Fe_3O_4 nanoparticles have been conjugated to HRP to introduce peroxidase activity in a number of applications, including commercially available magnetic enzyme-linked immunosorbent assay (ELISA) kits, demonstrates that the presence of this activity has so far been ignored. The fact that Fe_3O_4 MNPs have peroxidase-like activity poses the potential for novel applications and so we characterized this activity, taking HRP as a comparison.

RESULTS

Fe_3O_4 MNPS CATALYSE THE OXIDATION OF PEROXIDASE SUBSTRATES

We first prepared Fe_3O_4 MNPs of different sizes (30, 150 and 300 nm). The Fe_3O_4 MNPs appeared spherical and homogeneous and were of the expected size (Fig. 1a). We found that the Fe_3O_4 MNPs of all sizes catalysed the reaction of the substrate 3,3,5,5-tetramethylbenzidine (TMB) in the presence of H_2O_2 to produce a blue colour reaction (Fig. 1b), with maximum absorbance at 652 nm. Like enzymatic peroxidase activity, such as observed for the commonly used enzyme HRP, this colour reaction was quenched by adding H_2SO_4 (see the reference to TMB at www.sigmaaldrich.com).

To further characterize the peroxidase-like activity of the Fe_3O_4 MNPs, we repeated the experiments using other peroxidase substrates in place of TMB, including di-azo-aminobenzene (DAB) and *o*-phenylenediamine (OPD). Figure 1b shows that the Fe_3O_4 MNPs not only catalysed oxidation of TMB producing a blue

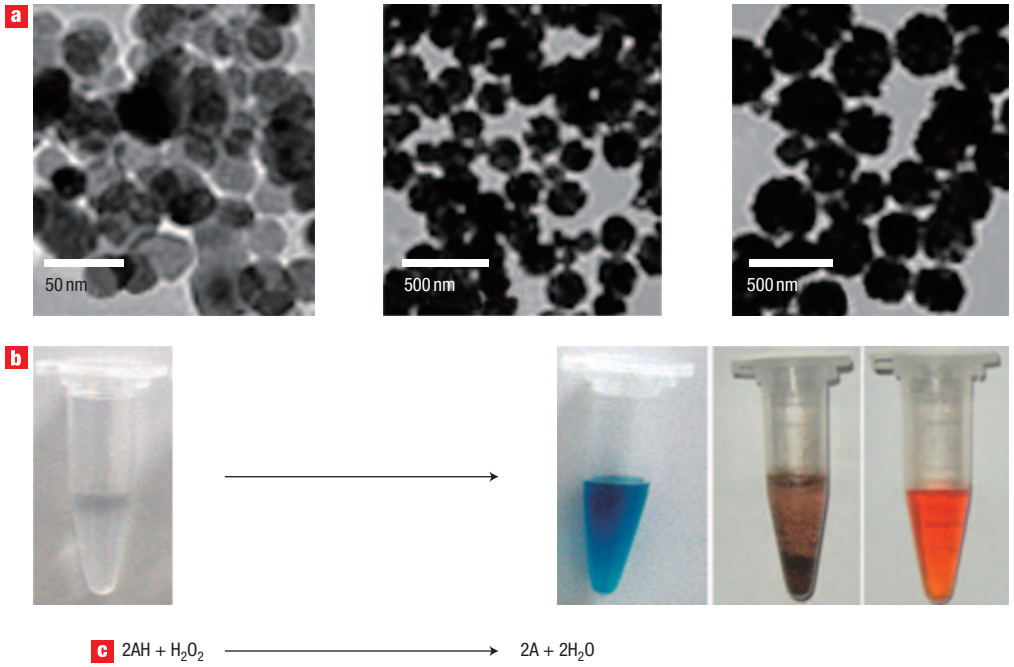

Figure 1 Fe_3O_4 MNPs show peroxidase-like activity. a, TEM images of Fe_3O_4 MNPs of different sizes. **b**, The Fe_3O_4 MNPs catalyse oxidation of various peroxidase substrates in the presence of H_2O_2 to produce different colour reactions. **c**, Scheme of the mechanism of catalysis by Fe_3O_4 MNPs. AH represents the substrate, which is a hydrogen donor.

colour, but also DAB to give a brown colour and OPD to give an orange colour. These results indicate that the Fe_3O_4 MNPs have peroxidase-like activity towards typical peroxidase substrates (Fig. 1c).

H_2O_2, PH, TEMPERATURE AND SIZE DEPENDENCE

The catalytic activity of the Fe_3O_4 MNPs is, like HRP, dependent on pH, temperature and H_2O_2 concentration. We measured the peroxidase-like activity of 300-nm Fe_3O_4 MNPs while varying the pH from 1 to 12, the temperature from 25 °C to 60 °C, and the H_2O_2 concentration from 0.001 to 2.26 M and compared the results with the activity found in HRP over the same range of parameters. The optimal pH and temperature were approximately pH 3.5 and 40 °C, which are very similar to the values for HRP (Fig. 2a,b). Thus, we adopted pH 3.5 and 40 °C as standard conditions for subsequent analysis of Fe_3O_4 MNP activity. We found that the Fe_3O_4 MNPs required a H_2O_2 concentration two orders of magnitude higher than HRP to reach the maximal level of peroxidase activity. However, further increase in the H_2O_2 concentration inhibited the peroxidase-like activity of the Fe_3O_4 MNPs, as is observed for the enzyme catalysed reaction (Fig. 2c).

As the properties of nanoscale materials are often dependent on size, we studied the catalysis of Fe_3O_4 MNPs of different sizes (300, 150 and 30 nm). Interestingly, the Fe_3O_4 MNPs showed different levels of activity towards TMB in the order 30 nm > 150 nm > 300 nm (Fig. 2d); that is, the smaller the size, the higher the catalytic activity. This phenomenon may be due to the smaller nanoparticles having a greater surface-to-volume ratio to interact with substrates.

ACTIVITY IS DUE TO INTACT MNPS NOT IONS LEACHING INTO SOLUTION

It is important to rule out the possibility that the observed activity is caused by leaching of iron ions into acidic solution. To test this, we incubated MNPs in the standard reaction buffer (pH 3.5) for 10 min (the time taken to observe a plateau in the observed activity) and then removed the MNPs from solution with a magnet. We then compared the activity of the leaching solution with that of MNPs under the same conditions. As shown in Fig. 3, the leaching solution had no activity, showing that the observed peroxidase-like activity is due to intact MNPs.

We also analysed the iron content of the leaching solution using atomic absorption spectroscopy. MNPs of size 300 nm were incubated under the standard reaction conditions and allowed to settle out of solution over a period of 30 min. The Fe content in the supernatant was then analysed, giving a value of 21.2 ($\pm$0.7 $\mu g\,l^{-1}$), which is two orders of magnitude lower than the concentration required for the Fenton reaction[20]. This further demonstrates that the observed reaction cannot be attributed to leaching of iron ions into solution, but occurs on the surface of the MNPs.

Table 1 Comparison of the kinetic parameters of Fe_3O_4 MNPs and HRP. [*E*] is the enzyme (or MNP) concentration, K_m is the Michaelis constant, V_{max} is the maximal reaction velocity and K_{cat} is the catalytic constant, where $K_{cat} = V_{max}/[E]$.

	[*E*] (M)	Substrate	K_m (mM)	V_{max} ($M\,s^{-1}$)	K_{cat} (s^{-1})
Fe_3O_4 MNPs	11.4×10^{-13}	TMB	0.098	3.44×10^{-8}	3.02×10^{4}
Fe_3O_4 MNPs	11.4×10^{-13}	H_2O_2	154	9.78×10^{-8}	8.58×10^{4}
HRP	2.5×10^{-11}	TMB	0.434	10.00×10^{-8}	4.00×10^{3}
HRP	2.5×10^{-11}	H_2O_2	3.70	8.71×10^{-8}	3.48×10^{3}

REACTION MECHANISM

To investigate the mechanism of the peroxidase activity of the Fe_3O_4 MNPs, we determined apparent steady-state kinetic parameters for the reaction. As noted above, the nanoparticle-catalysed

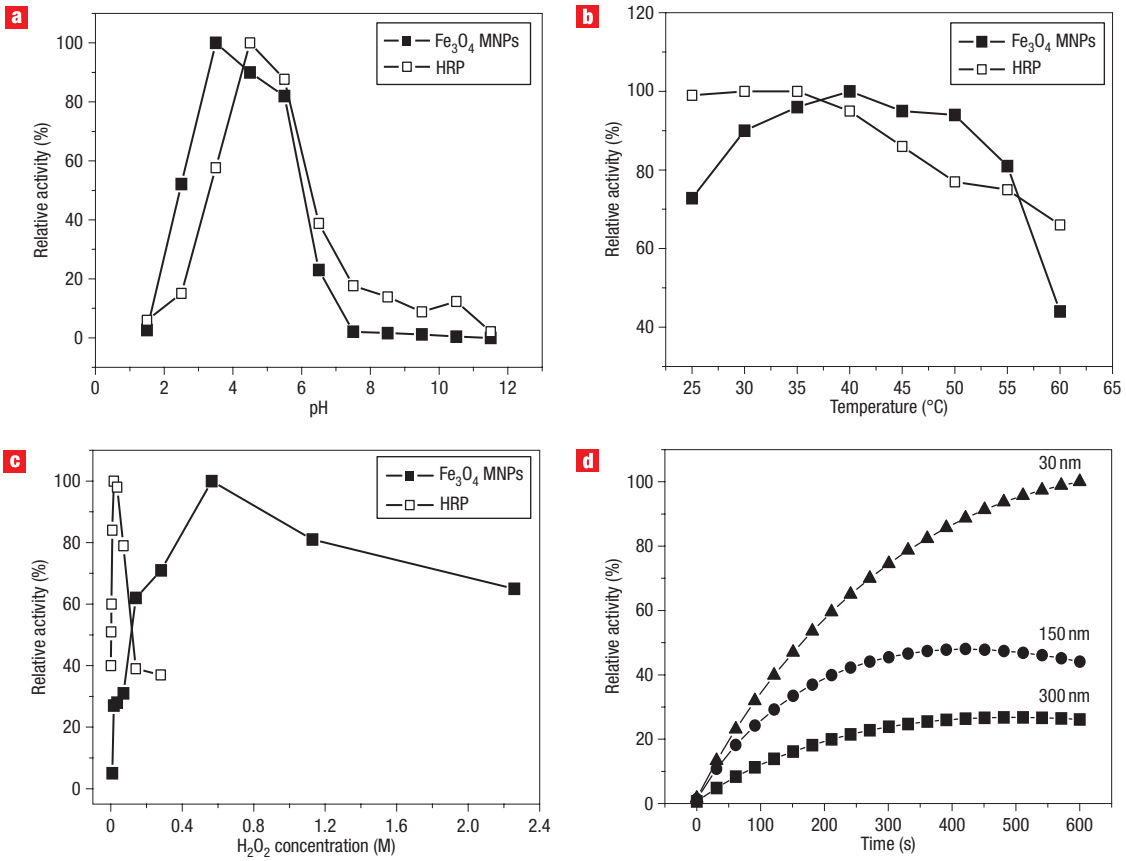

Figure 2 The peroxidase-like activity of the Fe_3O_4 MNPs is pH, temperature, H_2O_2 concentration and size dependent. Experiments were carried out using 20 μg MNPs or 0.50 ng HRP in a reaction volume of 0.5 ml, in 0.2 M NaAc buffer, with 816 μM TMB as substrate. The H_2O_2 concentration was 530 mM for MNPs and 8.8 mM for HRP. The pH was 3.5, and the temperature was 40 °C, unless otherwise stated. The maximum point in each curve (**a**–**c**) was set as 100%. **a**, Fe_3O_4 MNPs and HRP show an optimal pH of 3.5–4.5. **b**, Fe_3O_4 MNPs and HRP show an optimal temperature around 30–40 °C. **c**, Fe_3O_4 MNPs require a higher H_2O_2 concentration than HRP to reach maximal peroxidase activity. **d**, Under the same conditions, smaller Fe_3O_4 MNPs show higher peroxidase-like activity.

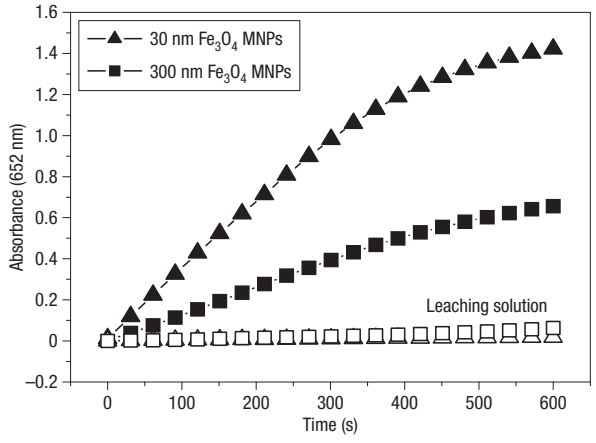

Figure 3 Demonstration that Fe_3O_4 activity does not result from iron leaching. Fe_3O_4 MNPs (30 nm and 300 nm, as indicated) were incubated in the pH 3.5 reaction buffer for 600 s, and then removed using a magnet. The activity of the leaching solution was then compared to that of the MNPs. Conditions were as described in Fig. 2.

reaction is inhibited at high H_2O_2 concentrations, as is the enzyme-catalysed reaction. However, within the suitable range of H_2O_2 concentrations, typical Michaelis–Menten curves were observed for both Fe_3O_4 MNPs (Fig. 4a,b) and HRP (Fig. 4c,d). The data were fitted to the Michaelis–Menten model to obtain the parameters shown in Table 1. The apparent K_m value of the Fe_3O_4 MNPs with H_2O_2 as the substrate was significantly higher than that for HRP (Table 1), consistent with the observation that a higher concentration of H_2O_2 was required to observe maximal activity for the MNPs. The apparent K_m value of the Fe_3O_4 MNPs with TMB as the substrate was about four times lower than HRP (Fig. 4a,c, and Table 1), suggesting that the Fe_3O_4 MNPs have a higher affinity for TMB than HRP. At the same molar concentration, the Fe_3O_4 MNPs showed a level of activity 40 times higher than HRP. This may be due to the fact that an HRP molecule has only one iron ion[21], in contrast to the surface of an Fe_3O_4 MNP. The presence of ferrous and ferric ions in the nanoparticles is likely to be the key to their catalysis.

To investigate the catalytic roles of Fe^{2+} and Fe^{3+} ions in Fe_3O_4 MNPs, we treated the particles with either $NaIO_4$ or $NaBH_4$. We found that treatment with the reducing agent $NaBH_4$, which increases the proportion of Fe^{2+} ions, increased the activity of the nanoparticles, whereas the oxidizing agent $NaIO_4$, which

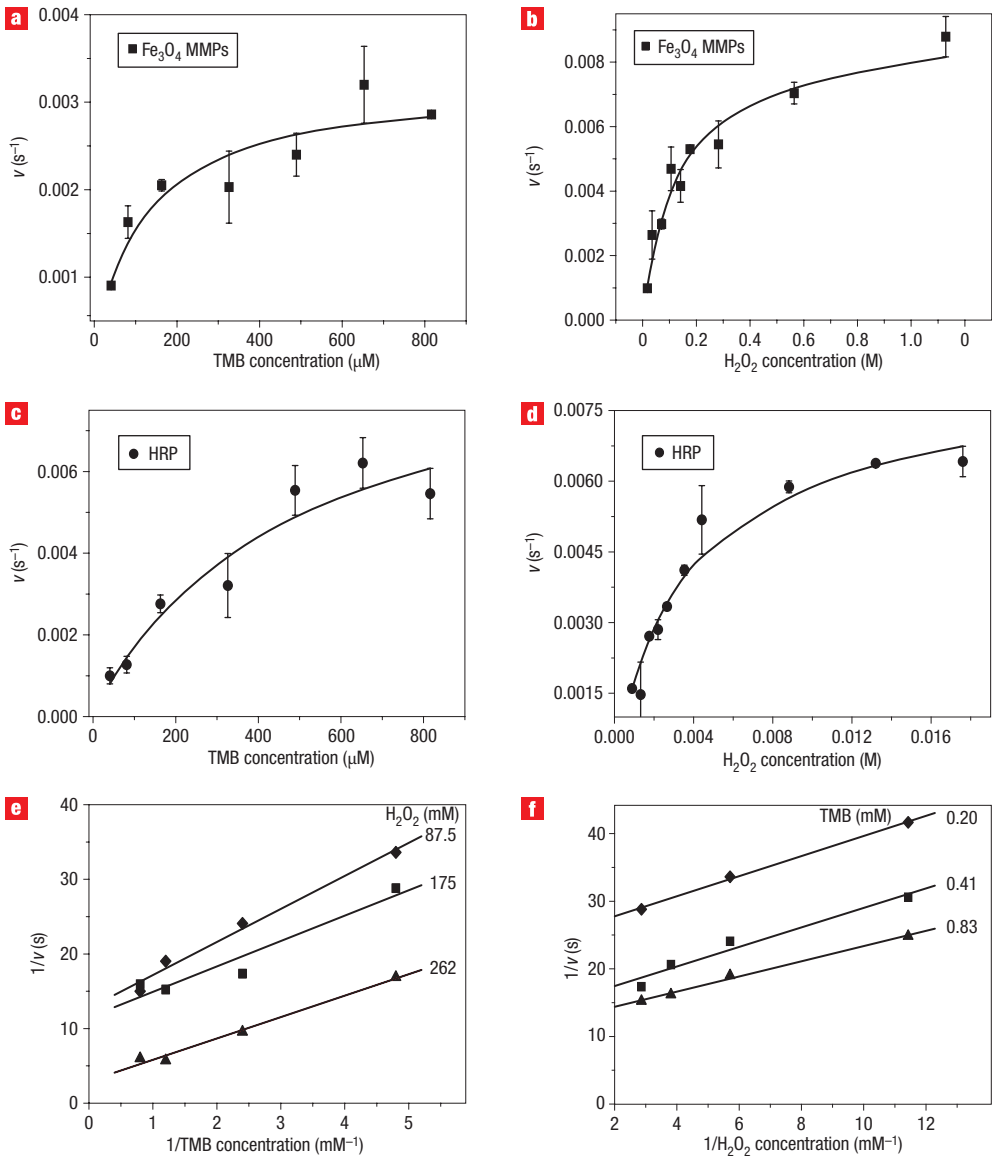

Figure 4 Steady-state kinetic assay and catalytic mechanism of Fe_3O_4 MNPs. a–d, The velocity (v) of the reaction was measured using 20 μg Fe_3O_4 MNPs (**a**,**b**) or 0.5 ng HRP (**c**,**d**) in 500 μl of 0.2 M NaAc pH 3.5 at 40 °C. Error bars shown represent the standard error derived from three repeated measurements. **a**,**c**, The concentration of H_2O_2 was 530 mM (Fe_3O_4 MNPs) or 8.8 mM (HRP) and the TMB concentration was varied. **b**,**d**, The concentration of TMB was 816 μM and the H_2O_2 concentration was varied. **e**,**f**, Double-reciprocal plots of activity of Fe_3O_4 MNPs at a fixed concentration of one substrate versus varying concentration of the second substrate for H_2O_2 and TMB. The y-axis values are observed absorbance values.

decreases the proportion of Fe^{2+} ions, decreased the activity (see Supplementary Information, Fig. S1). This suggests that Fe^{2+} ions may play a dominant role in the catalytic peroxidase-like activity of Fe_3O_4 MNPs.

To further investigate the mechanism of catalysis of Fe_3O_4 MNPs, we measured their activity over a range of TMB and H_2O_2 concentrations. Figure 4e,f shows double reciprocal plots of initial velocity versus one substrate concentration, obtained for a range of concentrations of the second substrate. The slope of the lines is parallel, which is characteristic of a ping-pong mechanism, as is observed for HRP (ref. 22). This then indicates that, as for HRP, the MNPs bind and react with the first substrate, releasing the first product before reacting with the second substrate.

COMPARISON OF ROBUSTNESS OF PEROXIDASE ACTIVITY OF Fe_3O_4 MNPS AND HRP

Because Fe_3O_4 MNPs are an inorganic nanomaterial, they are expected to be more stable than the enzyme HRP. To test this, we first incubated both HRP and the nanoparticles at a range of temperatures (4, 16, 25, 37, 50, 70, 90 °C) and a range of values of pH (0–12) for 2 h, and then measured their activities under standard conditions (pH 3.5 and 40 °C). The Fe_3O_4 MNPs were indeed found to remain stable over a wide range of pH from 1 to 12, and temperatures from 4 to 90 °C. In contrast, the enzyme HRP did not show any activity after treatment at pH lower than 5 or temperatures greater than 40 °C (Fig. 5a,b). The robustness of Fe_3O_4 MNPs makes them suitable for a broad range of applications in the biomedicine and environmental chemistry fields.

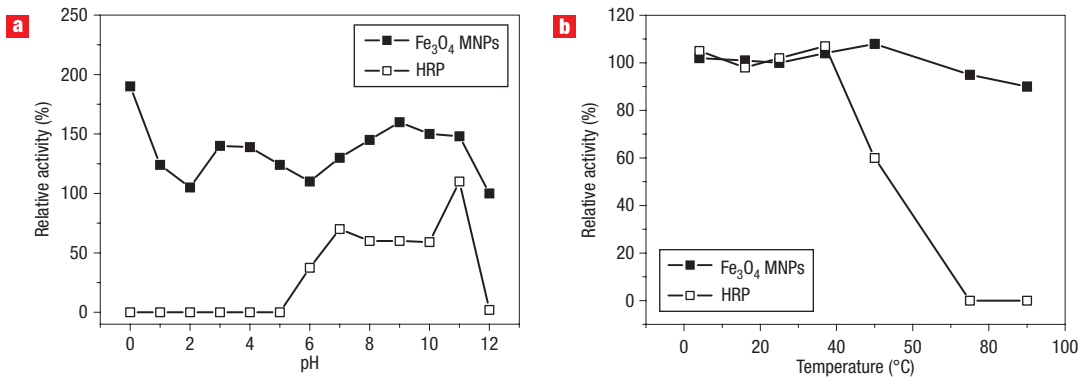

Figure 5 Comparision of the stability of Fe_3O_4 MNPs and HRP. a, Fe_3O_4 MNPs and HRP were first incubated at a range of values of pH from 0 to 12 for 2 h and then their peroxidase activities were measured under standard conditions. **b**, Fe_3O_4 MNPs and HRP were first incubated at a range of temperatures between 4 and 90 °C for 2 h and then the peroxidase activitiy was measured under standard conditions.

PRODUCTION OF TRIPLE-FUNCTION Fe_3O_4 MNPS AND THEIR APPLICATION IN AN IMMUNOASSAY

Based on our finding, we developed two immunoassays using the intrinsic dual functionality of the Fe_3O_4 MNPs as a peroxidase and magnetic separator. In these assays, we first modified the Fe_3O_4 MNPs (30 nm) with different compounds including SiO_2, 3-aminopropyltriethoxysilane (APTES), polyethylene glycol (PEG) or dextran to make them biocompatible. We observed that the enzyme activity of the modified Fe_3O_4 MNPs decreased after modification (Fig. 6a). A number of factors may influence the extent to which surface-modifying groups shield the surface from the substrate and hence affect activity, such as size and density of packing of the modifying groups and the thickness of the coating layer. For a given type of modifying group, variation in the modification protocol can produce coats of different thickness[23–25]. Under the conditions used in this study (see Methods), we observed that the highest degree of activity was maintained after dextran modification (Fig. 6a). We therefore used dextran to modify the Fe_3O_4 MNPs before immobilizing the antibody or protein of interest on the modified surface of the Fe_3O_4 MNPs.

In the first immunoassay (Fig. 6b), we immobilized protein A on Fe_3O_4 MNPs and used this in place of an enzyme-conjugated secondary antibody. As for conventional ELISA, we coated a plate with hepatitis B virus surface antigen (preS1), and then incubated the plate with anti-HBV preS1 antibody. After several washes, non-specific binding was removed. The Fe_3O_4 MNPs with immobilized protein A and the substrate TMB were then added, so that protein A bound to the primary anti-preS1 antibody and Fe_3O_4 MNPs catalysed a colour reaction in the presence of H_2O_2. The reaction was measured using an ELISA reader at 652 nm. This demonstrates that the intrinsic peroxidase-like activity of the MNPs can still be detected after surface modification. In this scenario, the magnetic properties of the MNPs could potentially be used for recovery or recycling of the MNPs.

In the second immunoassay (Fig. 6c), we combined the two intrinsic properties of Fe_3O_4 MNPs, namely magnetism and peroxidase activity, in a novel capture–detection immunoassay. First, an antibody to cardiac troponin I (TnI), a well-known biomarker for myocardial infarction, was immobilized on the Fe_3O_4 MNPs. The antibody-labelled Fe_3O_4 MNPs were then mixed with serum, allowing capture of the target TnI in the sample. The TnI captured by Fe_3O_4 MNPs was easily separated from the sample using a magnet. After washing off contaminants, the MNPs with target bound were transferred onto a plate coated with another anti-TnI antibody. After washing off non-bound MNPs, the substrate TMB was added in the presence of H_2O_2 and the bound Fe_3O_4 MNPs catalysed a colour reaction, which was measured using an ELISA reader at 652 nm. As shown in Fig. 6c, the concentration of TnI in the sample correlated with the colour reaction.

These assays demonstrate the versatility and power of Fe_3O_4 MNPs as both a capture agent and a detection tool, due to their intrinsic dual functionality. This can be compared with traditional magnetic-ELISA, in which Fe_3O_4 MNPs capture targets and an additional step is required to introduce a secondary antibody carrying, for example, HRP to allow detection. This new method is easier, faster and more economical, and provides greater sensitivity. Further, the intrinsic peroxidase-like activity of Fe_3O_4 MNPs should be taken into account when they are used in standard magnetic ELISA: conjugation of the secondary antibody to HRP for detection is likely to lead to high background. In fact, it was this observation that led us to discover the peroxidase-like activity of the Fe_3O_4 MNPs.

DISCUSSION

In this study, we provide the first report that Fe_3O_4 MNPs possess intrinsic peroxidase-like activity comparable to that of an enzyme-catalysed reaction by demonstrating that (1) Fe_3O_4 MNPs catalysed the reaction of different peroxidase substrates such as TMB, DAB and OPD to give the same colour changes as HRP; (2) the peroxidase-like activity of Fe_3O_4 MNPs was also H_2O_2, pH and temperature dependent; (3) catalysis by Fe_3O_4 MNPs showed typical Michaelis–Menten kinetics; and (4) catalysis by Fe_3O_4 MNPs was consistent with a ping-pong mechanism.

In general, the enzyme activity of proteins is lost after exposure to extremes of pH and high temperature, and proteins are also susceptible to digestion by proteases, which are ubiquitous in the environment. To reduce time and cost of production and purification of enzymes, there is increasing interest in enzyme mimetics, which are more robust than proteins and easier or more economical to produce. For example, peroxidase mimetics including haemin, haematin, porphyrin, haemaglobin, and cyclodextrin[26–34] have been studied and applied in environmental chemistry, such as to remove phenols from wastewater[35]. Further, metallic nanoparticles have been conjugated to horseradish peroxidase and applied as a sensor for H_2O_2 (ref. 36) or as a

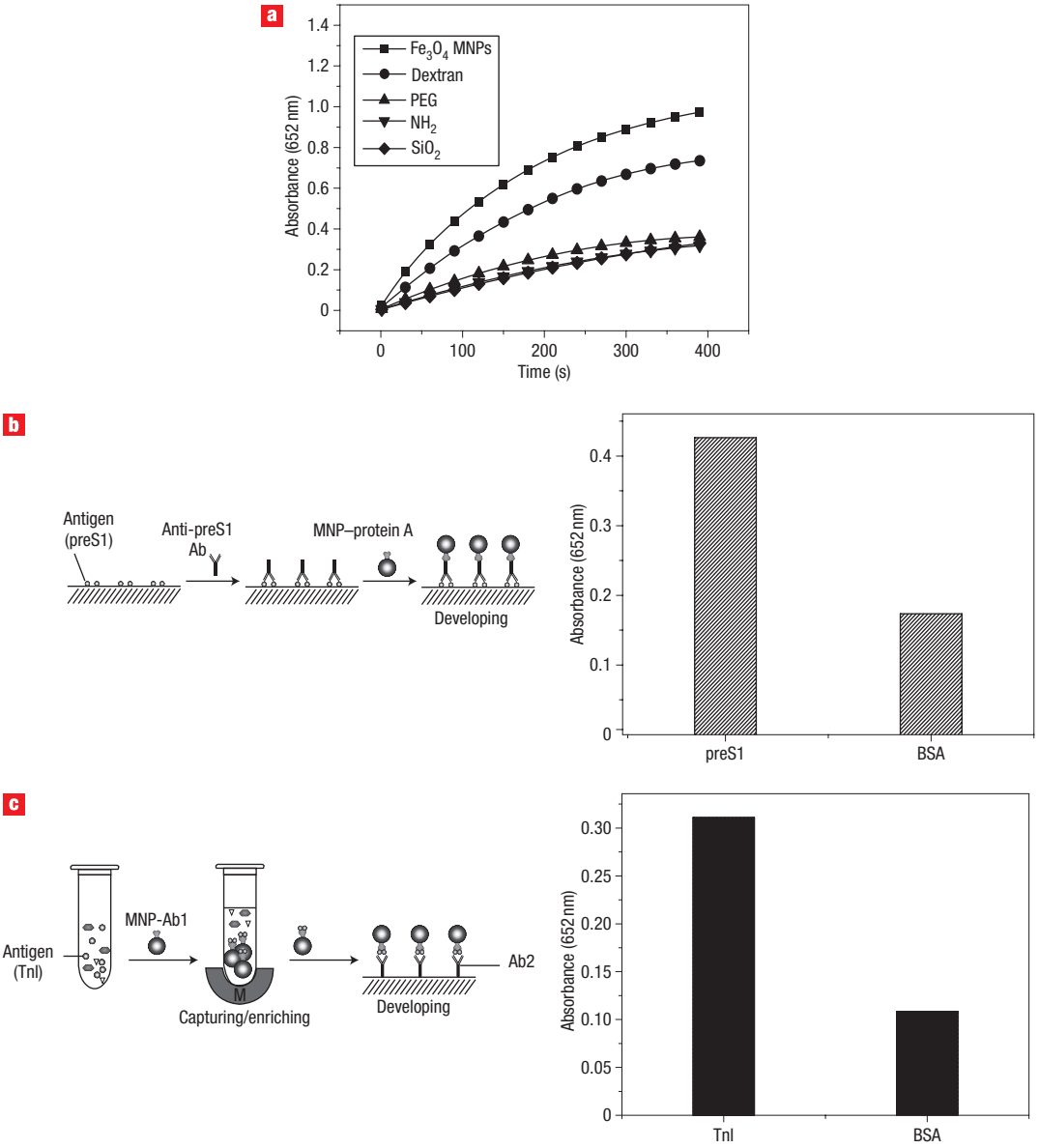

Figure 6 Immunoassays based on the peroxidase activity of Fe_3O_4 magnetic nanoparticles. a, The catalytic activity of Fe_3O_4 MNPs modified with different groups. **b**, Fe_3O_4 MNPs-based immunoassay. HBV preS1 antigen was recognized by anti-preS1 antibody and detected by Fe_3O_4 MNPs conjugated to protein A, which specifically binds to the Fc fragment of the antibody. **c**, A capture–detection immunoassay. Antibody-modified Fe_3O_4 MNPs were used to capture and separate the target TnI in the sample. This complex was reacted with the secondary anti-TnI antibody, which was coated on the plate, and a colour reaction developed when the substrate TMB was added in the presence of H_2O_2.

biocatalyst[14]. Our findings demonstrate that Fe_3O_4 MNPs can be used as a peroxidase mimetic.

Further, Fe_3O_4 MNPs are highly effective as a catalyst, with a higher binding affinity for the substrate TMB than HRP and a 40-fold higher level of activity at the same molar concentration of catalyst. Importantly, Fe_3O_4 MNPs have the additional property of being magnetic, which allows them to be recovered for recycling, or to be used as a capture agent when appropriately modified.

Taken together, these results demonstrate that Fe_3O_4 MNPs act as a robust and effective peroxidase mimetic, as well as a versatile capture and detection tool. Our findings open up a wide range of new potential applications of Fe_3O_4 MNPs in environmental chemistry, biotechnology and medicine.

METHODS

MATERIALS

TMB, DAB, OPD, CDI and HRP (EC 1.11.1.7) were purchased from Sigma-Aldrich $FeCl_3{\cdot}6H_2O$, ethylene glycol and NaAc were purchased from Beijing Chemical Reagents. Two types of anti-TnI antibody and sample containing TnI were provided by Biosino Bio-Technology and Science.

SYNTHESIS AND MODIFICATION OF Fe_3O_4 MNPS

Fe_3O_4 MNPs with diameters of approximately 150 nm and 300 nm were prepared according to the solvothermal method and 30 nm Fe_3O_4 MNPs were prepared by the co-precipitation method. The size distribution of these MNPs has been characterized previously[37,38]. Fe_3O_4 MNPs with dextran were prepared using the same procedure but adding dextran. Silica coating of MNPs was

performed using an improved Ströber method, which produces a relatively thick silica shell, as described[25]. For silica coating and amino modification of Fe_3O_4 MNPs, 26 mg Fe_3O_4 nanoparticles were mixed with 20 ml 2-propanol and 40 ml ethanol. Then, 0.5 ml deionized water and 1.5 ml ammonia solution (25% by wt) were consecutively added to the reaction mixture. Under continuous mechanical stirring, APTES and TEOS (tetraethoxysilane) with different ratios (0 or 1:4, total 400 μl) were added into the reaction solutions. The reactions were allowed to proceed at room temperature for 8 h. After the coating reaction, the core–shell nanostructures were separated from the reaction medium by centrifuging at ~3,000 r.p.m., and dispersed into ethanol. The separation procedure was performed several times. To confirm the reproducibility of our findings, Fe_3O_4 MNPs were produced in two independent labs, and the behaviour of the MNPs from the two sources was found to be consistent.

KINETIC ANALYSIS

Unless otherwise stated, steady-state kinetic assays were carried out at 40 °C in a 1.5-ml tube with 20 μg Fe_3O_4 MNPs (~2.7×10^8 nanoparticles) or 0.5 ng HRP (~6×10^9) in 500 μ l of reaction buffer (0.2 M NaAc, pH 3.5) in the presence of 530 mM H_2O_2 for Fe_3O_4 MNPs or 8.8 mM for HPR, using 816 μM TMB as the substrate. The reaction buffer used for OPD was 0.2 mol l^{-1} $Na_2HPO_4{\cdot}12H_2O$ and 0.1 mol l^{-1} citric acid; and for DAB was 0.05 M Tris-HCl, 0.15 M NaCl, pH 7.5. Immediately after the substrates were added, colour reactions were observed.

All the reactions were monitored in timescan mode at 652 nm using a Hitachi UV2010 spectrophotometer. The apparent kinetic parameters were calculated based on the function $v = V_{max} \times [S]/(K_m + [S])$, where v is the initial velocity, V_{max} is the maximal reaction velocity, $[S]$ is the concentration of substrate and K_m is the Michaelis constant.

To investigate the mechanism, assays were carried out under standard reaction conditions as described above by varying concentrations of TMB at a fixed concentration of H_2O_2 or vice versa.

ANTIBODY-IMMOBILIZED Fe_3O_4 MNPS

Before coupling with antibody, the dextran-modified Fe_3O_4 MNPs were activated by incubation with $NaIO_4$ (2 mg ml^{-1}) at 37 °C for 20 min, washed three times with 0.2 mol l^{-1} NaAc, pH 4.4, and suspended in 0.1 mol l^{-1} $NaHCO_3$, pH 9.6. The Fe_3O_4 MNPs were then incubated with 100 μg ml^{-1} anti-TnI antibody at 4 °C overnight. $NaBH_4$ was added to a final concentration of 2 mg ml^{-1} to stop the coupling reaction. After washing with PBS three times, the antibody-coupled Fe_3O_4 MNPs were stored at 4 °C for the capture–detection immunoassay.

Received 26 February 2007; accepted 20 July 2007; published 26 August 2007.

References

1. Bergemann, C. *et al.* Magnetic ion-exchange nano- and microparticles for medical, biochemical and molecular biological applications. *Magn. Magn. Mater.* **194,** 45–52 (1999).
2. Safarik, I. *et al.* Magnetic techniques for the isolation and purification of proteins and peptides. *Biomagn. Res. Technol.* **2,** 7 (2004).
3. Morishita, N. *et al.* MNPs with surface modification enhanced gene delivery of HVJ-E vector. *Biochem. Biophys. Res. Commun.* **334,** 1121–1126 (2005).
4. Ito, A. *et al.* Construction and delivery of tissue-engineered human retinal pigment epithelial cell sheets using magnetite nanoparticles and magnetic force. *Tissue Eng.* **11,** 489–496 (2005).
5. Brahler, M. *et al.* Magnetite-loaded carrier erythrocytes as contrast agents for magnetic resonance imaging. *Nano Lett.* **6,** 2505–2509 (2006).
6. de Vries, I. J. *et al.* Magnetic resonance tracking of dendritic cells in melanoma patients for monitoring of cellular therapy. *Nature Biotechnol.* **23,** 1407–1413 (2005).
7. Denis, M. C. *et al.* Imaging inflammation of the pancreatic islets in type 1 diabetes. *Proc. Natl Acad. Sci. USA* **101,** 12634–12639 (2004).
8. Chemla, Y. R. *et al.* Ultrasensitive magnetic biosensor for homogeneous immunoassay. *Proc. Natl Acad. Sci. USA* **97,** 14268–14272 (2000).
9. Hirsch, L. R. *et al.* Nanoshell-mediated near-infrared thermal therapy of tumors under magnetic resonance guidance. *Proc. Natl Acad. Sci. USA* **100,** 13549–13554 (2003).
10. Yoon, T. J. *et al.* MNPs as a catalyst vehicle for simple and easy recycling. *New J. Chem.* **27,** 227–229 (2003).
11. Stevens, P. D. *et al.* Superparamagnetic nanoparticle-supported catalysis of Suzuki cross-coupling reactions. *Org. Lett.* **7,** 2085–2088 (2005).
12. Hu, A. *et al.* Magnetically recoverable chiral catalysts immobilized on magnetite nanoparticles for asymmetric hydrogenation of aromatic ketones. *J. Am. Chem. Soc.* **127,** 12486–12487 (2005).
13. Tsang, S. C. *et al.* Magnetically separable, carbon-supported nanocatalysts for the manufacture of fine chemicals. *Angew. Chem. Int. Edn* **43,** 5645–5649 (2004).
14. Yang, H. H. *et al.* Magnetite-containing spherical silica nanoparticles for biocatalysis and bioseparations. *Anal. Chem.* **76,** 1316–1321 (2004).
15. Jun, C. H. *et al.* Demonstration of a magnetic and catalytic Co@Pt nanoparticle as a dual-function nanoplatform. *Chem. Commun.* 1619–1621 (2006).
16. Henriksen, A. *et al.* The structures of the horseradish peroxidase C-ferulic acid complex and the ternary complex with cyanide suggest how peroxidases oxidize small phenolic substrates. *J. Biol. Chem.* **274,** 35005–35011 (1999).
17. Kvaratskhelia, M. *et al.* Purification and characterization of a novel class III peroxidase isoenzyme from tea leaves. *Plant. Physiol.* **114,** 1237–1245 (1997).
18. Kariya, K. *et al.* Purification and some properties of peroxidases of rat bone marrow. *Biochim. Biophys. Acta.* **911,** 95–101 (1987).
19. Mathy-Hartert, M. *et al.* Purification of myeloperoxidase from equine polymorphonuclear leucocytes. *Can. J. Vet. Res.* **62,** 127–132 (1998).
20. Hsueh, C. L., Huang, Y. H., Wang, C. C. & Chen, C. Y. Degradation of azo dyes using low iron concentration of Fenton and Fenton-like system. *Chemosphere* **58,**1409–1414 (2005).
21. Yamada, H. *et al.* Proton balance in conversions between five oxidation–reduction states of horseradish peroxidases. *Arch. Biochem. Biophys.* **165,** 728–738 (1974).
22. Porter, D. J. T. & Bright J. H. The mechanism of oxidation of nitroalkanes by horseradish peroxidase. *J. Biol. Chem.* **258,** 9913–9924 (1982).
23. Bruce, I. J. *et al.* Synthesis, characterisation and application of silica–magnetite nanocomposites. *J. Magn. Magn. Mater.* **284,** 145–160 (2004).
24. Yang, Y. D. *et al.* Influence of preparation parameters and characterization of nano-compound superparamagnetic iron oxide particle in dextran system. *J. Inorg. Mater.* **20,** 226–229 (2005).
25. Sun, Y. K. *et al.* An improved way to prepare superparamagnetic magnetite–silica core–shell nanoparticles for possible biological application. *J. Magn. Magn. Mater.* **285,** 65–70 (2005).
26. Zhu, Q. Z. *et al.* Fluorescence immunoassay of alpha-1-fetoprotein with hemin as a mimetic enzyme labeling reagent. *Anal. Chem.* **362,** 537–540 (1998).
27. Zhang, G. F. *et al.* Hematin as a peroxidase substitute in hydrogen peroxide determinations. *Anal. Chem.* **64,** 517–522 (1992).
28. Bonar-Law, R. P. *et al.* Polyol recognition by a steroid-capped porphyrin enhancement and modulation of misfitguest binding by added water or methanol. *J. Am. Chem. Soc.* **117,** 259–271 (1995).
29. Wang, Q. L. *et al.* Highly sensitive fluorescent enhance assay for ascorbic acid. *Anal. Chem.* **28,** 1229–1232 (2000).
30. Liu, Z. H. *et al.* Highly sensitive spectrofluorimetric determination of hydrogen peroxide with β-cyclodextrin–hemin as catalyst. *Analyst* **124,** 173–176 (1999).
31. Ci, Y. X. *et al.* Chemiluminescence investigation of the interaction of metalloporphyrins with nucleic acids. *Anal. Chim. Acta.* **282,** 695–701 (1993).
32. Tie, J. K. *et al* Application of enzyme-field effect transistor sensor arrays as detectors in a flow-injection analysis system for simultaneous monitoring of medium components. Part II. Monitoring of cultivation processes. *Anal. Chim. Acta.* **300,** 25–31 (1995).
33. Cai, Y. X. *et al.* Fluorimetric mimetic enzyme immunoassay of methotrexate Fresenius. *Anal. Chem.* **349,** 317–319 (1994).
34. Zhu, C. Q. *et al.* Application of manganese–teasulfonatophthalocyanine as a new mimetic peroxidase in the determination of hydrogen peroxide in marine surface water samples with p-hydroxyphenglacetic acid as a substrate. *Anal. Sci.* **16,** 253–256 (2000).
35. Cheng, J. *et al.* Horseradish peroxidase immobilized on aluminium-pillared inter-layered clay for the catalytic oxidation of phenolic wastewater. *Water Res.* **40,** 283–290 (2006).
36. Ren, C. *et al.* Hydrogen peroxide sensor based on horseradish peroxidase immobilized on a silver nanoparticles/cysteamine/gold electrode. *Anal. Bioanal. Chem.* **381,** 1179–1185 (2005).
37. Deng, H. *et al.* Monodisperse magnetic single-crystal ferrite microspheres. *Angew. Chem. Int. Edn* **44,** 2782–2785 (2005).
38. Ma, M. *et al.* Size dependence of specific power absorption of Fe_3O_4 particles in AC magnetic field. *J. Magn. Magn. Mater.* **268,** 33–39 (2004).

Acknowledgements

We thank Sishen Xie and Chen Wang for helpful discussions. This work is partly supported by grants from the National Natural Science Foundation of China (NSFC) (90406020, 30670428), the Knowledge Innovation Program of the Chinese Academy of Sciences (kjcx-yw-m02, kjcx2-sw-h12), the Chinese Ministry of Sciences 973 Project (2006CB933204, 2006CB500703, 2006CB910901, 2006CB910903), and the Ministry of Education, Culture, Sports, Science and Technology (MEXT) of Japan.
Correspondence and requests for materials should be addressed to X.Y. or S.P.
Supplementary information accompanies this paper on www.nature.com/naturenanotechnology.

Author contributions

L. G., J. Zhuang, S. P. and X. Y. designed the research. L. G., J. Zhuang, J. F., D. Y. and J. Zhang performed the research. L. N., Y. Z., N. G., and T. W. contributed new reagents and analytic tools. L. G., J. Zhuang, J. Zhang and X. Y. analysed the data. L. G., S. P. and X. Y. wrote the paper. All authors discussed the results and commented on the manuscript.

Competing financial interests

The authors declare no competing financial interests.